

Axial loading during MRI influences T2-mapping values of lumbar discs: a feasibility study on patients with low back pain

Martin Nilsson^{1,4}  · K. Lagerstrand^{3,4} · I. Kasperska¹ · H. Brisby^{2,4} · H. Hebelka^{1,4}

Received: 12 February 2016/Revised: 23 May 2016/Accepted: 18 June 2016/Published online: 24 June 2016
© Springer-Verlag Berlin Heidelberg 2016

Abstract

Purpose To investigate whether axial loading of the spine during MRI (alMRI) instantaneously induces changes in biochemical disc features as reflected by altered quantitative T2 values in patients with chronic low back pain (LBP).

Methods T2 mapping was performed on 11 LBP patients (54 lumbar discs) during the conventional unloaded MRI and subsequent alMRI. Each disc was divided into five volumetric regions of interests (ROIs), anterior annulus fibrosus (AF) (ROI 1), the interface anterior AF-nucleus pulposus (NP) (ROI 2), NP (ROI 3), the interface NP-posterior AF (ROI 4), and the posterior AF (ROI 5). The mean T2 values for each ROI were compared between MRI and alMRI and correlated with degeneration grade (Pfirrmann), disc angle, and disc level.

Results With alMRI, T2 values increased significantly in the whole disc as well as in various parts of the disc with an increase in ROI 1–3 and a decrease in ROI 5. The changes in T2 values correlated to degeneration grade, changes in disc angle, and lumbar level.

Conclusion alMRI instantaneously induces T2-value changes in lumbar discs and is, thus, a feasible method to

reveal dynamic, biochemical disc features in patients with chronic LBP.

Keywords Chronic low back pain · Quantitative magnetic resonance imaging · T2 mapping · Disc degeneration · Axially loaded magnetic resonance imaging

Introduction

Non-specific chronic low back pain (LBP), associated with degeneration of the intervertebral disc (IVD), represents a major worldwide health issue with high costs in addition to severe individual consequences [1]. A major causality for non-specific LBP is assumed to be pathological pain signaling from the IVD [2–4] or the cartilaginous endplates [5, 6]. The pathophysiology behind chronic LBP is, however, still not elucidated, and clinical management is suffering from the absence of a reliable method that unequivocally points out which spinal structures causes the LBP [7–9].

Quantitative MRI methods, aiming for better understanding of the early processes of painful disc degeneration, are under development. Apart from T2 mapping, other quantitative methods that have been applied in clinically advanced settings include T1rho-imaging, T2*-mapping ('T2 star'), and ADC-mapping (apparent diffusion coefficient) [4, 6, 10–13]. In T2 mapping, voxel-specific T2-relaxation times (T2 values) are determined from a series of continually increasing echo times. In principle, T2 values correlate to the concentration of water molecules in a given tissue but are also influenced by the interaction of these water molecules with their molecular environment, notably the amount and orientation of collagenous fibers [14, 15]. T2 mapping improves the discrimination of disc structures and facilitates the assessment of the biochemical

✉ Martin Nilsson
martin.os.nilsson@vregion.se

¹ Department of Radiology, Sahlgrenska University Hospital, Göteborg, Sweden

² Department of Orthopaedics, Sahlgrenska University Hospital, Göteborg, Sweden

³ Department of Medical Physics and Techniques, Sahlgrenska University Hospital, Göteborg, Sweden

⁴ Institute of Clinical Sciences, Sahlgrenska Academy, University of Gothenburg, Göteborg, Sweden

composition of the IVD. T2 values have been shown to inversely correlate with degeneration grade, with the capacity to discriminate nucleus pulposus (NP) from annulus fibrosus (AF) [10, 11, 16–21].

Despite that T2 mapping provides an objective measure of degeneration, there are very few studies investigating the relationship between mechanical IVD properties and T2 values [20, 22]. In terms of studies on LBP patients, there is, to our knowledge, only one study addressing the issue [20]. Stelzeneder et al. investigated the effects of axial unloading of the spine in LBP patients and found significant alterations in intra-discal T2 values by unloading.

Chronic LBP is usually aggravated by axial loading of the spine [2, 3, 5], which is thought to be due to some kind of mechanical impairment inducing pain in the degenerated IVD or in the adjacent endplates. The method of axial loading during MRI (aMRI) in the supine position has previously been shown to aggravate pain in patients with chronic LBP, and to induce morphological disc changes [23]. To our knowledge, the effect on T2 values of lumbar IVDs by the application of axial load during MRI has not yet been investigated in patients.

The aim of the study was to investigate if aMRI is a feasible method to instantaneously induce changes in bio-dynamic disc features as reflected by altered T2 values in patients with chronic LBP.

Patients and methods

Study participants

Eleven patients with chronic LBP, clinically severe enough to be considered for surgery, were referred from the spine surgery unit at Sahlgrenska University Hospital, Gothenburg, Sweden. None of the patients presented any radicular nerve symptoms. None of the patients had any previous disc surgery or any contraindications for MRI. The study group consisted of seven men (mean age 41 years, range 25–51 years) and four women (mean age 44 years, range 25–69 years). Out of 55 lumbar discs, one L5–S1 disc was excluded because of stabilized sacralization, resulting in a total of 54 analyzed discs in 11 patients. The study was conducted according to the Declaration of Helsinki. Ethical approval was given by the Regional Ethics Review Board at the Västra Götaland Region, and oral and written informed consent was obtained from all participants.

Magnetic resonance imaging

All patients were subjected to an MRI examination performed on a Siemens Magnetom Aera 1.5 T scanner (Erlangen, Germany) consisting of an initial supine protocol

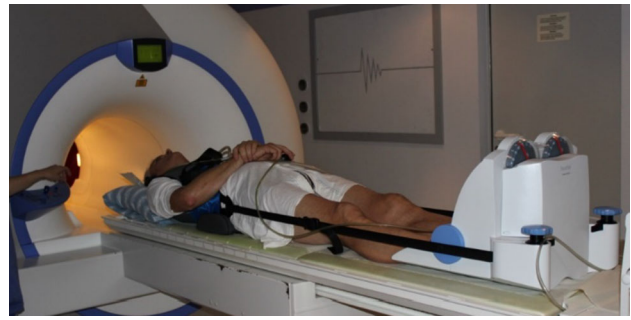


Fig. 1 DynaWell compression device. A patient in the MRI scanner with the compression device. A harness is attached with straps to a foot-plate, applying an axially directed load corresponding to 50 % of the body weight. To prevent flexion and, instead, facilitate a normal lordosis associated with the upright standing position, a small cushion was placed under the lumbar spine

(unloaded MRI) (20 min) followed by an immediate identical repeat supine protocol with the addition of axial loading (aMRI) (20 min). The T2 mapping sequence was included last in the protocols and, hence, T2 mapping with and without axial load was spaced by 20 min in time. All scans were made between 10:00 a.m. and 1:00 p.m. The aMRI was performed with a DynaWell compression device (DynaWell diagnostics AB, Las Vegas, NV, USA) (Fig. 1) [24]. The protocol constituted of TSE T1- and T2-weighted (W) sequences in the sagittal plane, an axial TSE T2W-sequence, and an SE T2-mapping sequence in the sagittal plane (Table 1).

Measurements

The discs of L1–S1 were classified according to the Pfirrmann method [25]. Lumbar lordosis (from superior endplate of L1 to superior endplate of S1) and disc angles (Fig. 2) were measured on midsagittal T1-W images. IVD segmentation (volumetric delineation) was made on fused sagittal T1- and T2-mapping sequences on the Syngovia (Siemens) image processing software, because the addition of T1 signal improves the resolution of the T2 mapping images (Fig. 2). The images were then multiplanar reformatted into non-overlapping slices of 10 mm, and three such slices were used in the analysis on each disc level, one midsagittal and two parasagittal, thus covering 30 mm of the median disc width in total. Each disc was further divided into five equal parts in the sagittal plane (Fig. 3). This was done by the initial measurement in millimeters of the individual discs in the midsagittal plane. In each sagittal slice, five regions of interest (ROI) were delineated along the disc contours by application of the polygonal ROI tool. The sagittal length of each ROI was drawn along a ruler tool marking corresponding to one-fifth of the known total midsagittal length of the disc. The ROIs were thus generated to represent anterior AF (ROI 1), anterior

Table 1 MRI and aMRI protocol details

	NSA (<i>n</i>)	Flip (α)	TR (ms)	TE (ms)	Slice (mm)	Matrix	FOV (cm)
FSE T1 sag	2	150	480	9	3.5	320 × 320	30 × 30
FSE T2 sag	1	150	3500	95	3.5	384 × 38	430 × 30
FSE TS ax	2	150	5330	97	3.5	320 × 320	20 × 20
SE T2-map	1	180	1400	11/89	3.5	256 × 256	22 × 22

NSA number of signal averages, *Flip* (α) flip angle, *TR* repetition time, *TE* echo time, *Slice* slice thickness, *Matrix* matrix size, *FOV* field of view

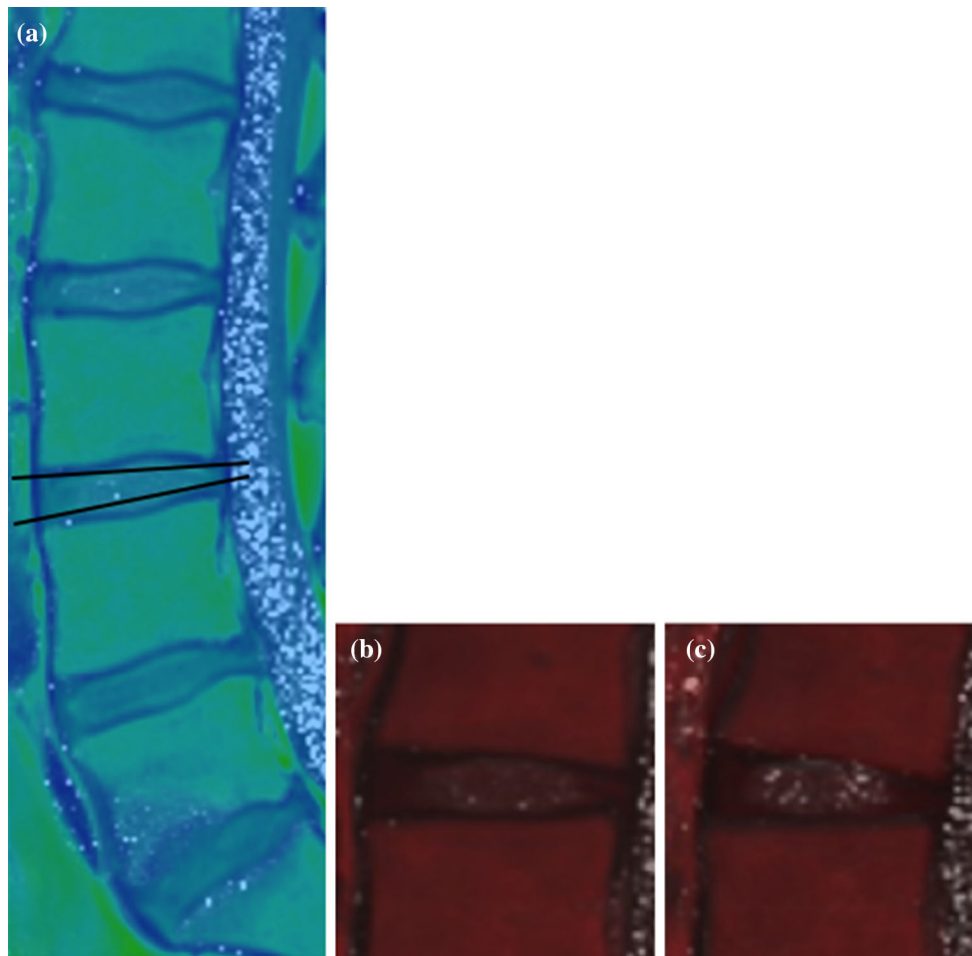


Fig. 2 Fused T1-/T2-mapping images. **a** Example of the color setting used for the segmentation of the disc, as it was deemed to satisfactorily enhance the disc borders. The *lines* along the endplates of the L3–L4 disc have been added to illustrate how disc angles were assessed. **b** Displaying a non-degenerated L2–L3 disc with a *color*

setting visually enhances the intra-discal bright areas denoting voxels with particularly high T2 values. **c** With aMRI, an increase in disc angle and changes in the T2 signal of the nucleus pulposus are appreciable

AF-NP border (ROI 2), NP (ROI 3), posterior NP-AF border (ROI 4), and posterior AF (ROI 5), respectively. In this fashion, a total of 15 separate volumetric ROIs of each disc were delineated (Fig. 3). Mean T2 values (ms), standard deviations of the means (ms), and ROI-areas (mm²) were recorded for each separate volume. Mean T2 values of all three adjacent sagittal slices were calculated regarding each of the five anteroposterior parts of the discs,

resulting in the mean T2 values of five sagittal volumes per disc level. With the exception of the Pfirrmann grading, all measurements were repeated in identical fashion for the aMRI images. All measurements were made by a radiology resident (MN) who also performed intra-observer analysis after a minimum interval of 1 month, blinded to the original results. Blinded inter-observer analysis was performed by a radiology specialist (HH).

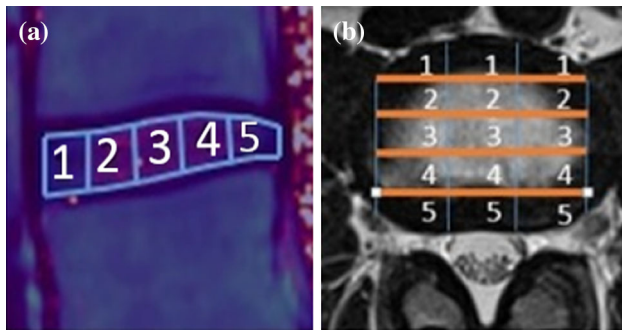


Fig. 3 Conceptual sagittal and axial illustration of the disc segmentation. **a** The sagittal length of each ROI corresponds to 20 % of the total midsagittal length of the disc. The ROIs are delineated by the respective cranial and caudal endplates. **b** Separate measurements were made in each of three consecutive, non-overlapping midsagittal, and parasagittal 10 mm multiplanar reconstructed slices. These were added to mean values for each of the ROI 1–5 in the sagittal plane. Thus, each ROI 1–5 represents mean T2 values of the median 30 mm in the coronal (frontal) plane. A total of 15 volumetric measurements were made per disc

Statistical analysis

The description of data was expressed in terms of the mean and standard deviation (SD). A parametric paired *t* test was used for comparison between differences in T2 values between unloaded MRI and aMRI. Non-parametric

Spearman rank correlation and parametric Pearson’s product-moment correlation were used for the evaluation of how differences in T2 values were associated to differences in IVD angle and Pfirrmann grade. Bivariate Pearson’s analysis was also performed to correlate induced changes in lordosis with induced changes in disc angles. Reliability of quantitative measurements for both intra- and inter-rater agreement was performed using intra-class correlation coefficients (ICC) with 95 % confidence intervals. ICC model 2 was used with single measurements to determine consistency in agreement. The coefficients were interpreted according to Landis and Koch [26]. All tests were two-sided, and statistical significance was set as *p* < 0.05. Data were analyzed using IBM SPSS Statistics for Windows, Version 22.0 (Armonk, NY: IBM Corp, USA).

Results

Changes in T2 values

Comparison between unloaded MRI and aMRI showed a significant increment in T2 value of the whole disc, from 58 to 60 ms (*p* < 0.05). Stratified according to disc level, this change was significant on the L2–L3 and L5–S1 levels (Table 2). There were significant alterations in T2 values for

Table 2 Differences in T2 values between unloaded MRI and aMRI for discs stratified according to respective disc level

	Mean	SD	95 % confidence interval of the difference		<i>p</i> value
			Lower	Upper	
L1–L2	–2.7	16	–7.1	1.6	0.213
L2–L3	–5.1	17.7	–10.4	–0.8	0.023
L3–L4	–2.1	19.6	–7.4	3.3	0.442
L4–L5	–0.4	9.2	–2.9	2	0.723
L5–S1	–1.9	6.6	–3.7	0	0.048

The bold values represent *p* values (=expression of significance)
SD standard deviation

Table 3 Comparison between T2 values (ms) for unloaded MRI and aMRI in the five different ROIs

	Unloaded MRI (<i>N</i> = 54)		aMRI (<i>N</i> = 54)		Difference unloaded MRI–aMRI				
	Mean	SD	Mean	SD	95 % CI				<i>p</i> value
					Mean	SD	Lower	Upper	
ROI 1	30.8	5.9	35.0	10	–4.2	8.3	–6.4	–1.9	0.001
ROI 2	61.9	29.3	70.6	36.8	–8.7	16.3	–13.2	–4.3	0.000
ROI 3	80.9	37.2	87.2	46.6	–6.3	18.2	–11.2	–1.4	0.014
ROI 4	74.9	34.2	73.9	33.4	0.92	13.7	–2.8	4.6	0.624
ROI 5	41.0	13.3	35.5	10.6	5.6	11.1	2.5	8.6	0.001

Each ROI represents one-fifth of the sagittal length of the disc. The width of each ROI represents the median 30 mm of the disc. ROI 1 is regarded to represent the anterior annulus fibrosus (AF), ROI 2: border zone between anterior AF and nucleus pulposus (NP), ROI 3: NP, ROI 4: border zone between NP and posterior AF, and ROI 5: posterior AF

ROI region of interest, SD standard deviation, CI confidence interval

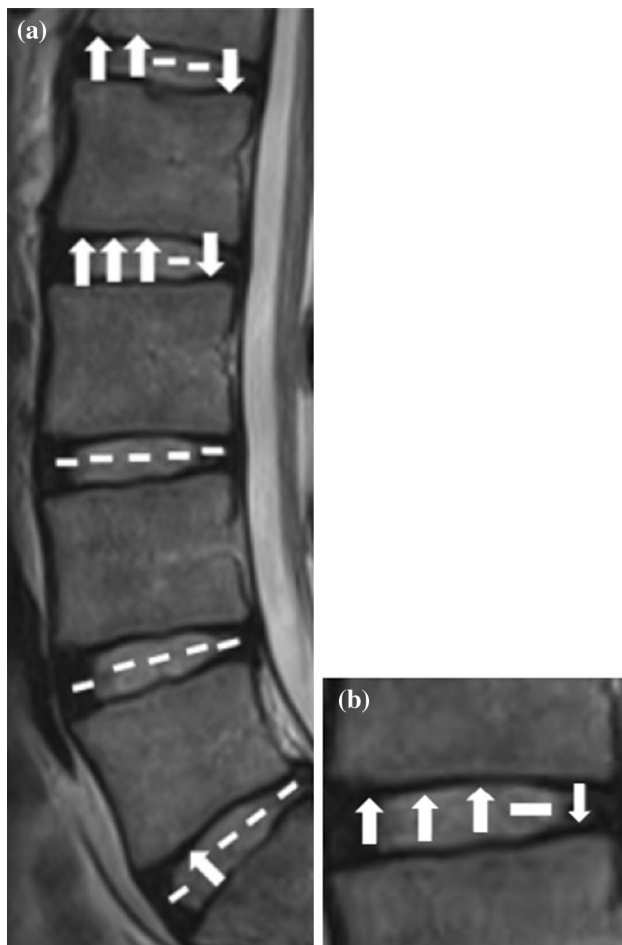


Fig. 4 Illustrations of changes in T2 values induced with aMRI. **a** Illustration of changes in T2 values according to disc levels comparing unloaded MRI with aMRI. **b** Illustration of changes in T2 values comparing unloaded MRI and aMRI when all 54 discs were analyzed together. A significant increase is designated by *up arrows* and decrease by *down arrows*. Non-significant changes are designated by *lines*

all ROIs, except for ROI 4, between unloaded MRI and aMRI (Table 3). When the different ROI's were analyzed with respect to disc levels, significant increments in T2 values with

aMRI were seen in ROI 1 and 2 of the L1–L2 and L2–L3 levels ($p < 0.05$) with concomitant reductions in ROI 5 on the same disc levels ($p < 0.05$). In addition, increments in T2 values were also seen with aMRI in ROI 3 of the L2–L3 level ($p < 0.05$) and ROI 2 of the L5–S1 level ($p < 0.05$). For all other ROIs, there were no statistically significant differences between unloaded MRI and aMRI (Fig. 4).

Correlation to Pfirrmann grades

When graded according to Pfirrmann, 3 discs were grade 1, 27 grade 2, 16 grade 3, and 8 grade 4. No grade 5 discs were found in the study group. No analysis of correlation was performed between the singular Pfirrmann grades and T2 values, due to the limited number of discs with the highest Pfirrmann grades. Instead, Pfirrmann grades were dichotomized into two groups; I–II and III–IV, respectively. Absolute T2 values were higher in the Pfirrmann I–II group compared with the III–IV group in all ROIs ($p < 0.001$) (Table 4). Increments in T2 values with aMRI were more pronounced in the I–II group in ROI 1 ($p < 0.001$), ROIs 2–3 ($p < 0.04$) with a concomitantly more pronounced reduction in ROI 5 ($p < 0.05$), compared with group III–IV (Table 4).

Correlations to lumbar lordosis and changes in disc angles

The aMRI induced an increment of the mean lumbar lordosis of $11^\circ (\pm 5^\circ)$ and a mean increment of 2.2° (SD 2.8, range 15) of the IVD angle. Furthermore, the induced changes in IVD angles correlated to concurrent changes in T2 values in ROI 1–3 ($p < 0.05$, $k = 0.3$) and in ROI 5 (<0.01 , $k = -0.4$).

Intra- and inter-observer analysis

ICC for the intra-observer analysis ranged between 0.85 and 1.0 for ROI 2–5, both for unloaded MRI and for

Table 4 Absolute aMRI T2 values (ms) and differences in T2 values between unloaded MRI and aMRI with comparison made between Pfirrmann I–II and III–IV groups

	Mean aMRI T2 values					Change in T2 values between unloaded MRI–aMRI				
	Pfirrmann grade		Mean difference	<i>p</i> value	95 % CI	Pfirrmann grade		Mean difference	<i>p</i> value	95 % CI
I and II (<i>n</i> = 30)	III and IV (<i>n</i> = 24)	I and II (<i>n</i> = 30)				III and IV (<i>n</i> = 24)				
ROI 1	38.9 (11.0)	30.1 (5.3)	8.9	<0.001	4.2–3.5	–7.89 (8.68)	0.43 (4.94)	–8.3	<0.001	–12.3 to –4.3
ROI 2	91.7 (36.2)	44.5 (12.9)	47.2	<0.001	31.3–63.1	–13.1 (19.9)	–3.5 (7.24)	–9.6	0.020	–17.5 to –1.6
ROI 3	114 (44.9)	54.0 (17.1)	60.4	<0.001	40.5–80.3	–10.6 (22.4)	–1.2 (8.8)	–9.5	0.042	–18.5 to –0.4
ROI 4	94.9 (28.3)	48.0 (16.5)	46.9	<0.001	33.5–60.2	1.8 (17.3)	–0.2 (7.2)	1.9	0.58	–5.1 to 9.0
ROI 5	40.2 (11.2)	29.5 (5.9)	10.7	<0.001	5.5–15.9	8.3 (12.8)	2.6 (7.2)	5.7	0.047	0.09 to 11.3

ROI regions of interest, CI confidence interval, standard deviations in parentheses

alMRI, and between 0.68 and 0.79 for ROI 1. Inter-observer analysis showed ICC 0.87–1.0 for all ROIs for both unloaded MRI and alMRI, with the exceptions of ROI 1 (0.79) and ROI 5 (0.43) for alMRI [26].

Discussion

The main findings in this study were that alMRI instantaneously induced an increment in T2 values in the disc as a whole, and that this was most pronounced in the anterior AF and the NP coupled with a concomitant reduction in the posterior AF. Furthermore, the instant changes in T2 values correlated with parameters related to the degree of degeneration, as the Pfirrmann grading and change in IVD angle.

These results most probably reflected structural and biochemical disc alterations induced by the axial load, explained by dynamic effects on the spatial distribution of intra-discal water. However, the differences in mean T2 values between unloaded MRI and alMRI should not only reflect a redistribution of water molecules. Rather it might be a measure of the state of global biochemical disc structure, influenced by proteoglycans and collagen. Collagen causes well-known restriction in the mobility of water molecules through chemical interactions, and this effect on T2 relaxation time shortening is variable secondary to the orientation of the fibers in relation to the magnetic field [6, 14, 15].

The fact that T2 values increase in the anterior disc regions with concomitant decreases in posterior AF seems logical considering that in addition to axial load, the lumbar spine is extended during alMRI, with both increments in lordosis and IVD angle, resulting in higher load on posterior spinal structures, such as posterior AF. It seems likely that this increment of posterior load redistributes water molecules anteriorly in the disc, possibly into clefts in the anterior AF or in the NP, or into posterior annular fissures. The relative impact on T2 values by hydrodynamic distributions and structural disc composition within the disc, respectively, is substantially unknown and needs to be further explored. Irrespectively, the results show that this novel method is sensitive enough to depict such alterations instantaneously.

There were differences in T2 value changes between the various IVD levels in this study, but because of the small cohort, no general conclusions could be made regarding the impact of specific IVD levels. Theoretically, one may expect that the IVD position in relation to the center of the spinal load influences the degree of mechanically mediated biochemical reaction when forces are applied. The observed alMRI-induced T2-value changes were most pronounced in the upper lumbar spine levels. This might, however, also be explained by the fact that IVD

degeneration tends to be less pronounced there [27]. The changes in this study were, indeed, also most evident in relatively mildly degenerated discs (Table 4), which has also been shown to be the case in the prior, scarce, literature on loading-related T2 value changes in LBP patients [20]. Furthermore, the extent of changes in T2 values in the various ROIs correlated with changes in IVD angles suggesting that more rigid lumbar segments are less prone to react structurally/biochemically to applied axial load [3]. Overall, it seems plausible that the correlations between T2 value changes and segmental position, degeneration grade, and flexibility might simply represent different expressions of the same biochemical condition.

The absolute T2 values in this study and the variations related to AF and NP are in concordance with larger studies probing the correlations of quantitative T2 values to IVD histology and states of degeneration [10, 11, 16–18, 20, 21]. Slighter variations between studies can be explained by the fact that neither selection of study participants nor measuring methods have been strictly standardized. The fashion of volumetric ROI acquisition used in the current study, which enables the majority of the disc to be included, has not been used in other studies. To avoid partial volume averaging effects with paraspinal tissues, the most lateral millimeters of the disc could not be included in the ROIs. Still, previous studies are limited by smaller ROI volumes, such as one 4–5 mm midsagittal slice [10, 16, 19], two 5 mm parasagittal slices [11, 20, 21], or a single axial 3 mm slice [18], with substantial risks of losing important information in the peripheral disc regions. This aspect seems important when effects from axial loading are studied as increases in disc pressure may force gelatinous NP content into radial and circumferential AF fissures, i.e., into peripheral disc regions, or even out of the disc entirely.

Interestingly, in the study by Stelzeneder et al. [20], 48 LBP patients were subjected to two repeat supine MRI scans performed after upright position, thus achieving a situation of axial spinal unloading. In their study, T2 values in ROI 2 (anterior AF-NP border zone) decreased, while T2 values in ROI 5 (posterior AF) increased, which seem congruous with our results. However, incongruous to our findings, they found no differences when all ROIs were summated on a global disc level, which might be explained by the lack of peripheral ROI volumes in their study. It also appears plausible that biochemical responses will be more rapid when instantaneous active load is applied as compared to the more gradual and slow responses that can be assumed to occur when axial load is relieved passively.

Compared with supine alMRI, the use of upright position, being a more physiological approach, might be more revealing, possibly with added clinical value. Recently, Splendiani et al. reported, in a large study material, that

upright MRI revealed morphological changes in the forms of disc protrusions, spinal canal stenosis, segmental translational movements, and lumbar lordosis in a majority of the patients when compared to supine MRI [28]. Presumably, this would translate into significant changes in T2 values, as well. In the present study, supine aMRI was, however, chosen to keep a controlled position of the patient.

Limitations

Diurnal variations in T2 values are known to occur with decreasing T2 values in the nuclear region [29] and increasing T2 values in the annular region as the day progresses [30]. A standardized examination time focused on the morning instead of noon would have been preferable. The fact that significant changes were seen in the cohort even after ambulant, physiological loading of the spine might, however, be seen as proof of the methods robustness. Further limitations in this study are inherent to its small size, which restricts conclusions about validity and clinical utility. On the other hand, as a feasibility study, the results encourage further exploration.

Conclusion

The results show that T2 mapping combined with aMRI is a feasible method to reveal dynamical IVD properties and expressions of the internal biochemical disc architecture. Changes in T2 values were instantaneously induced with aMRI in the whole disc as well as in various disc parts with an increment in the anterior AF and the NP and a concomitant reduction in the posterior AF. For the evaluation of clinical usefulness, larger studies comparing LBP patients with controls are encouraged. This may clarify whether aMRI combined with T2 mapping also has the capacity to discover patterns specific to painful degenerated IVD.

Acknowledgments The study was supported by a regional Grant under the ALF agreement, number 428161 to HB, and by a grant to HH from Gothenburg Medical Society. The sponsors of the study had no influence on the analysis and interpretation of data; nor in the writing of the report. The authors would like to thank the MRI staff at Molndal Hospital, Gothenburg, Sweden, for the pleasant cooperation.

Compliance with ethical standards

Conflict of interest None.

References

- Dagenais S, Caro J, Haldeman S (2008) A systematic review of low back pain cost of illness studies in the US and internationally. *Spine J* 8:8–20. doi:10.1016/j.spinee.2007.10.005
- Bogduk N, Aprill C, Derby R (2013) Lumbar discogenic pain: state-of-the-art review. *Pain Med* 14:813–836. doi:10.1111/pme.12082
- Raj PP (2008) Intervertebral disc: anatomy–physiology–pathophysiology–treatment. *Pain Pract* 8:18–44. doi:10.1111/j.1533-2500.2007.00171.x
- Samartzis D, Borthakur A, Belfer I, Bow C, Lotz JC, Wang HQ, Cheung KM, Carragee E, Karppinen J (2015) Novel diagnostic and prognostic methods for disc degeneration and low back pain. *Spine J* 15:1919–1932. doi:10.1016/j.spinee.2014.09.010
- Lotz JC, Fields AJ, Liebenberg EC (2013) The role of the vertebral end plate in low back pain. *Glob Spine J* 3:153–164. doi:10.1055/s-0033-1347298
- Fields AJ, Han M, Krug R, Lotz JC (2015) Cartilaginous end plates: quantitative MR imaging with very short echo times–orientation dependence and correlation with biochemical composition. *Radiology* 274:482–489. doi:10.1148/radiol.14141082
- Chou R, Fu R, Carrino JA, Deyo RA (2009) Imaging strategies for low-back pain: systematic review and meta-analysis. *Lancet* 373:463–472. doi:10.1016/S0140-6736(09)60172-0
- Endean A, Palmer KT, Coggon D (2011) Potential of magnetic resonance imaging findings to refine case definition for mechanical low back pain in epidemiological studies: a systematic review. *Spine* 36:160–169. doi:10.1097/BRS.0b013e3181cd9adb
- Manchikanti L, Glaser SE, Wolfer L, Derby R, Cohen SP (2009) Systematic review of lumbar discography as a diagnostic test for chronic low back pain. *Pain Physician* 12:541–559
- Wang YX, Zhao F, Griffith JF, Mok GS, Leung JC, Ahuja AT, Yuan J (2013) T1rho and T2 relaxation times for lumbar disc degeneration: an in vivo comparative study at 3.0-Tesla MRI. *Eur Radiol* 23:228–234. doi:10.1007/s00330-012-2591-2
- Welsch GH, Trattng S, Paternostro-Sluga T, Bohndorf K, Goed S, Stelzeneder D, Mamisch TC (2011) Parametric T2 and T2* mapping techniques to visualize intervertebral disc degeneration in patients with low back pain: initial results on the clinical use of 3.0 Tesla MRI. *Skelet Radiol* 40:543–551. doi:10.1007/s00256-010-1036-8
- Hoppe S, Quirbach S, Mamisch TC, Krause FG, Werlen S, Benneker LM (2012) Axial T2 mapping in intervertebral discs: a new technique for assessment of intervertebral disc degeneration. *Eur Radiol* 22:2013–2019. doi:10.1007/s00330-012-2448-8
- Yu HJ, Bahri S, Gardner V, Muftuler LT (2015) In vivo quantification of lumbar disc degeneration: assessment of ADC value using a degenerative scoring system based on Pfirrmann framework. *Eur Spine J* 24:2442–2448. doi:10.1007/s00586-014-3721-0
- Boos N, Boesch C (1995) Quantitative magnetic resonance imaging of the lumbar spine. Potential for investigations of water content and biochemical composition. *Spine* 20:2358–2365 (discussion 2366)
- Mwale F, Iatridis JC, Antoniou J (2008) Quantitative MRI as a diagnostic tool of intervertebral disc matrix composition and integrity. *Eur Spine J* 17(Suppl 4):432–440. doi:10.1007/s00586-008-0744-4
- Takashima H, Takebayashi T, Yoshimoto M, Terashima Y, Tsuda H, Ida K, Yamashita T (2012) Correlation between T2 relaxation time and intervertebral disk degeneration. *Skelet Radiol* 41:163–167. doi:10.1007/s00256-011-1144-0
- Marinelli NL, Haughton VM, Anderson PA (2010) T2 relaxation times correlated with stage of lumbar intervertebral disk degeneration and patient age. *Am J Neuroradiol* 31:1278–1282. doi:10.3174/ajnr.A2080
- Watanabe A, Benneker LM, Boesch C, Watanabe T, Obata T, Anderson SE (2007) Classification of intervertebral disk degeneration with axial T2 mapping. *Am J Roentgenol* 189:936–942. doi:10.2214/AJR.07.2142

19. Blumenkrantz G, Zuo J, Li X, Kornak J, Link TM, Majumdar S (2010) In vivo 3.0-tesla magnetic resonance T1 ρ and T2 relaxation mapping in subjects with intervertebral disc degeneration and clinical symptoms. *Magn Reson Med* 63:1193–1200
20. Stelzeneder D, Kovacs BK, Goed S, Welsch GH, Hirschfeld C, Paternostro-Sluga T, Friedrich KM, Mamisch TC, Trattng S (2012) Effect of short-term unloading on T2 relaxation time in the lumbar intervertebral disc—in vivo magnetic resonance imaging study at 3.0 tesla. *Spine J* 12:257–264. doi:[10.1016/j.spinee.2012.02.001](https://doi.org/10.1016/j.spinee.2012.02.001)
21. Stelzeneder D, Welsch GH, Kovacs BK, Goed S, Paternostro-Sluga T, Vlychou M, Friedrich K, Mamisch TC, Trattng S (2012) Quantitative T2 evaluation at 3.0 T compared to morphological grading of the lumbar intervertebral disc: a standardized evaluation approach in patients with low back pain. *Eur J Radiol* 81:324–330. doi:[10.1016/j.ejrad.2010.12.093](https://doi.org/10.1016/j.ejrad.2010.12.093)
22. Maquer G, Brandejsky V, Benneker LM, Watanabe A, Verma-then P, Zysset PK (2014) Human intervertebral disc stiffness correlates better with the Otsu threshold computed from axial T2 map of its posterior annulus fibrosus than with clinical classifications. *Med Eng Phys* 36:219–225. doi:[10.1016/j.medengphy.2013.11.008](https://doi.org/10.1016/j.medengphy.2013.11.008)
23. Hebelka H, Brisby H, Hansson T (2014) Comparison between pain at discography and morphological disc changes at axial loaded MRI in patients with low back pain. *Eur Spine J* 23:2075–2082. doi:[10.1007/s00586-014-3408-6](https://doi.org/10.1007/s00586-014-3408-6)
24. Willen J, Danielson B (2001) The diagnostic effect from axial loading of the lumbar spine during computed tomography and magnetic resonance imaging in patients with degenerative disorders. *Spine* 26:2607–2614
25. Pfirrmann CW, Metzendorf A, Zanetti M, Hodler J, Boos N (2001) Magnetic resonance classification of lumbar intervertebral disc degeneration. *Spine* 26:1873–1878
26. Landis JR, Koch GG (1977) The measurement of observer agreement for categorical data. *Biometrics* 33:159–174
27. Cheung KM, Karppinen J, Chan D, Ho DW, Song YQ, Sham P, Cheah KS, Leong JC, Luk KD (2009) Prevalence and pattern of lumbar magnetic resonance imaging changes in a population study of one thousand forty-three individuals. *Spine* 34:934–940. doi:[10.1097/BRS.0b013e3181a01b3f](https://doi.org/10.1097/BRS.0b013e3181a01b3f)
28. Splendiani A, Perri M, Grattacaso G, Di Tunno V, Marsecano C, Panebianco L, Gennarelli A, Felli V, Varrassi M, Barile A, Di Cesare E, Masciocchi C, Gallucci M (2016) Magnetic resonance imaging (MRI) of the lumbar spine with dedicated G-scan machine in the upright position: a retrospective study and our experience in 10 years with 4305 patients. *Radiol Med (Torino)* 121:38–44. doi:[10.1007/s11547-015-0570-9](https://doi.org/10.1007/s11547-015-0570-9)
29. Silcox DH 3rd, Horton WC, Silverstein AM (1995) MRI of lumbar intervertebral discs. Diurnal variations in signal intensities. *Spine* 20:807–811 (**discussion 811–812**)
30. Ludescher B, Effelsberg J, Martirosian P, Steidle G, Markert B, Claussen C, Schick F (2008) T2- and diffusion-maps reveal diurnal changes of intervertebral disc composition: an in vivo MRI study at 1.5 Tesla. *J Magn Reson Imaging* 28:252–257. doi:[10.1002/jmri.21390](https://doi.org/10.1002/jmri.21390)